Journal of Pharmaceutical and Biomedical Analysis 57 (2012) 125–132

Contents lists available at SciVerse ScienceDirect

Journal of Pharmaceutical and Biomedical Analysis

journal homepage: www.elsevier.com/locate/jpba

Uricase-adsorbed carbon-felt reactor coupled with a peroxidase-modified carbon-felt-based H_2O_2 detector for highly sensitive amperometric flow determination of uric acid

Yue Wang [a], Yasushi Hasebe [b,*]

[a] School of Chemical Engineering, University of Science and Technology LiaoNing, 185 Qianshan Middle Road, High-tech Zone, Anshan, LiaoNing 114501, China
[b] Department of Life Science and Green Chemistry, Faculty of Engineering, Saitama Institute of Technology, 1690 Fusaiji, Fukaya, Saitama 369-0293, Japan

ARTICLE INFO

Article history:
Received 7 June 2011
Received in revised form 11 August 2011
Accepted 12 August 2011
Available online 22 August 2011

Keywords:
Flow-biosensor
Amperometry
Uricase
Peroxidase
Carbon-felt

ABSTRACT

Uricase (urate oxidase, UOx) was adsorbed onto a porous carbon-felt (CF) surface and the resulting UOx-adsorbed CF (UOx-CF) was successfully used as a column-type enzyme reactor coupled with a peroxidase-adsorbed CF-based bioelectrocatalytic H_2O_2 flow-detector to fabricate a flow-amperometric biosensor for uric acid. In this flow-biosensor system, H_2O_2 produced in the UOx-CF reactor was cathodically detected by horseradish peroxidase (HRP) and a thionine (Th)-coadsorbed CF (HRP/Th-CF)-based bioelectrocatalytic flow-detector at −0.05 V vs. Ag/AgCl. Various adsorption conditions of the UOx (i.e., pH of the adsorption solution, type and concentration of the buffer used as the adsorption solvent, UOx concentration and adsorption time) and the operational conditions of the UOx-CF and HRP/Th-CF-coupled flow-biosensor (i.e., carrier flow rate and carrier pH) were optimized to obtain highly sensitive, selective and stable peak current responses to uric acid. The analytical performance of the UOx-CF and HRP/Th-CF-coupled flow biosensor for uric acid was as follows: sensitivity, 0.25 μA/uM; linear range, 0.3–20 μM; lower detection limit, 0.18 μM; and sample throughput, ca. 30–90 samples/h. The resulting amperometric flow-biosensor for uric acid allowed the determination of uric acid in highly diluted body fluids (human serum and urine), and the analytical results obtained by the present biosensor were in fairly good agreement with those obtained by conventional enzyme-based spectrophotometry.

1. Introduction

Uric acid is a final product of the purine-metabolic pathway, and its detection is clinically important in the diagnosis of diseases caused by the disorder of purine biosynthesis and/or purine catabolism (e.g., gout, hyperuricema, Lesch–Nyhan syndrome and cardiovascular disease) [1].

Colorimetric methods based on the reduction ability of uric acid [2], adsorption chromatography [3] and high-performance liquid chromatography [4] have been employed for the detection of uric acid in body fluids. These methods, however, usually require time-consuming and relatively complicated procedures and relatively expensive equipment.

Uricase (EC. 1.7.3.3. urate oxidase, UOx) catalyzes the oxidative transformation of uric acid to allantoin with concomitant conversion of molecular oxygen to hydrogen peroxide [5]. Because UOx has a high specificity for uric acid, a UOx-based enzymatic assay has also been developed. In this case, enzymatically produced hydrogen peroxide is colorimetrically detected via a peroxidase–organic dye-coupling reaction [6]. A UOx-based fluorometric assay was also reported [7]. Again, however, these methods are not necessarily simple or convenient.

As compared to the methods mentioned above, UOx-based uric acid biosensors would be useful tools that could enable easy, simple and highly specific determination of uric acid [8–20]. In particular, a biosensor with a flow-injection mode (i.e., FIA-based biosensors) has the following advantages; (i) potential applicability for on-line analysis; (ii) possible high sample throughput; and (iii) the detectable concentration range and sensitivity can be easily altered by changing the sample injection volume. Therefore, the development of a highly functional, flow-type uric acid biosensor would be useful, especially for clinical analysis.

Carbon-felt (CF) is a microelectrode ensemble of micro-carbon fibers (ca. 7 μm diameter) with random three-dimensional structures [21]. CF has high conductivity and a large effective surface area (estimated to be 0.1–20 $m^2\ g^{-1}$), which allows large measurable current density and high electrolytic efficiency. In addition, the high porosity of CF (>90%) permits a low diffusion barrier of solution

* Corresponding author. Tel.: +81 48 585 6840; fax: +81 48 585 6840.
E-mail address: hasebe@sit.ac.jp (Y. Hasebe).

0731-7085/$ – see front matter © 2011 Elsevier B.V. All rights reserved.
doi:10.1016/j.jpba.2011.08.021

flow. Thus CF is very useful as the working electrode unit of electrochemical flow-through detectors [22–26]. As compared with other porous electrodes, CF has the following advantages: (i) inexpensive; (ii) physically stable; (iii) easily handled; and (iv) easily manufactured to arbitrary shapes.

Thus, biomolecule-immobilized CF is useful as a working electrode unit in electrochemical flow-biosensors. From this view point, we have been studying simple, convenient and effective protocols for enzyme immobilization onto the CF surface, and have developed enzyme-modified CF-based flow-biosensors [22–26]. Among various enzyme immobilization methods, physical adsorption is the simplest and most convenient. In previous studies, we reported that coadsorption of horseradish peroxidase (HRP) and thionine (Th) onto CF is effective for developing a highly sensitive bioelectrocatalytic flow-through detector for the amperometric determination of hydrogen peroxide [24–26]. In this case, the coadsorbed Th played an important role in facilitating the direct electron transfer between the HRP-active heme-center and the CF electrode surface [24–26]. Furthermore, the resulting HRP/Th-CF-based flow-through detector exhibited an excellent operational stability (repetitive 100 sample injection of 100 μM H_2O_2 induced no serious current decrease, and the RSD was 0.41–1.21% (n = 100) [24]. Strong interactions between the HRP molecule and the CF surface may contribute to this stable response. In addition, this HRP/Th-CF-based flow-through detector has excellent sensitivity toward H_2O_2 (detection limit, 0.02 μM) [26]. Therefore, the combination of this HRP/TH-CF-based H_2O_2 flow-detector and oxidases, which produce H_2O_2 during their catalyzed reactions, could enable the development of various flow-biosensors for the determination of the substrates of oxidases.

In this study, which is part of a series of studies on enzyme-modified CF-based flow-biosensors, we prepared UOx-adsorbed CF (UOx-CF) and combined it with the HRP/Th-CF-based H_2O_2 detector to fabricate an electrochemical FIA uric acid biosensor. As shown in Fig. 1, hydrogen peroxide produced enzymatically during the UOx-catalyzed oxidation of uric acid in the UOx-CF reactor is electrochemically detected by the HRP/Th-CF-based flow-through detector at −50 mV vs. Ag/AgCl. The main purpose of this study is as follows: (1) optimization of UOx adsorption conditions; (2) optimization of operational conditions; (3) evaluation of the analytical performance of the CF-based uric acid biosensor; and (4) determination of uric acid in human serum and urine using the present CF-based uric acid biosensor. If successful, the new system would be the first example of the combination of an oxidase-modified CF reactor and an HRP-based H_2O_2 flow-detector for fabrication of an oxidase/peroxidase coupled flow-biosensor.

2. Experimental

2.1. Reagents and materials

Horseradish peroxidase (HRP) [EC 1.11.1.7.; >100 units/mg] and uricase (UOx) [EC 1.7.3.3, from *candida* sp. 4.2 units/mg] were purchased from Wako Pure Chemicals and were used as received. Uric acid and 30% (v/v) hydrogen peroxide were also obtained from Wako Pure Chemicals. Thionine chloride (Th) was purchased from Tokyo Kasei Kogyo, Co. All of the other chemicals were of the highest grade available. A carbon-felt sheet (CF; GF-20-3F, which was prepared by pyrolysis of polyacrylonitrile at 2000 °C) was obtained from Nippon Carbon Ltd. The CF sheet (density 0.13 g/cm^3 and porosity greater than 90%) was cut into an appropriate size (i.e., 10 × 3 × 3 mm in size; weight ca. 12 mg; apparent volume 90 mm^3) and used as the immobilization (physical adsorption) matrix for the enzymes (i.e., UOx and HRP). The UOx-adsorbed CF (UOx-CF) was used as a flow-bioreactor, and the HRP and Th adsorbed CF (HRP/Th-CF) was used as a flow-through bioelectrocatalytic detector for H_2O_2. A standard solution of uric acid was prepared by dilution of uric acid with 0.1 M phosphate buffer (pH 8.0) as the carrier. An H_2O_2 standard solution was prepared by dilution of 30% H_2O_2 with buffer immediately prior to use. A 0.1 M phosphate buffer (prepared by using K_2HPO_4 and KH_2PO_4) was used as the standard sample and carrier solution. All of the solutions were prepared with doubly distilled water.

2.2. Preparation of enzyme-immobilized CF

Prior to surface modification, the CF was washed by ultrasonication for 15 min in distilled water. The UOx-adsorbed CF (UOx-CF) was prepared as follows: The CF was immersed in UOx-dissolved 0.1 M buffer solution at room temperature. Various adsorption conditions (i.e., pH, type of buffer, buffer concentration, UOx concentration and adsorption time) were optimized to obtain the largest peak current response to uric acid. Various buffers (pH 7.0, 0.1 M) [i.e., phosphate buffer, Britton–Robinson buffer, Tris–HCl buffer and borate buffer] were used as adsorption solutions for UOx. The HRP and Th-adsorbed CF (HRP/Th-CF) was prepared according to the methods previously reported by us [26]. Briefly, the CF was immersed in an HRP (0.033 mg ml) and Th (0.5 mM) mixed aqueous solution for 5 min under ultrasonic irradiation at 25 °C. These enzyme-adsorbed CFs were stored in 0.1 M phosphate buffer (pH 8.0) in the refrigerator at 4 °C when not in use.

2.3. Electrochemical measurements

In order to evaluate the interfacial properties of the UOx-adsorbed CF, cyclic voltammetry (CV) and electrochemical impedance spectroscopy (EIS) were performed with an electrochemical analyzer (ALS 6122a, USA). A deoxygenized 0.1 M phosphate buffer (pH 8.0, 15 ml) containing 0.25 mM hydroquinone was used as an electrolyte solution. Prior to measurement, pure nitrogen gas was bubbled into the solution for at least for 20 min to remove dissolved oxygen. The CV and EIS measurements were carried out under anaerobic conditions at room temperature with a conventional three electrodes system [i.e., the UOx-CF with platinum lead wire (0.5 mm of diameter) was the working electrode, a platinum wire (1 mm of diameter) was the counter electrode and Ag/AgCl (RE-1B, BAS, 3 M NaCl) was the reference electrode]. The applied potential was set at the formal potential of the hydroquinone/*p*-quinone redox system (*i.e.*, 0.05 V vs. Ag/AgCl at pH 8.0). The frequency ranged from 0.01 Hz to 10 kHz.

2.4. Flow injection detection of uric acid and H_2O_2 by the UOx-CF and HRP/Th-CF-coupled flow-biosensor

The flow injection analysis (FIA) system used in this study is essentially the same as the previously reported system, except for the insertion of the UOx-CF-bioreactor between the pump and the HRP/Th-CF-based H_2O_2 detector [24–26]. The schematic diagram of the UOx-CF-bioreactor and HRP/Th-CF-biodetector coupled FIA uric acid biosensor and the detection scheme for uric acid are shown in Fig. 1. The UOx-CF and HRP/Th-CF-coupled flow-uric acid biosensor is composed of a double syringe analytical pump (Sanuki Industry, SNK DX2000) with a six-way injection valve (SVM-6M2, SNK, 200 μL injection loop), the UOx-CF-based column-type-bioreactor, and the HRP/Th-CF-based bioelectrocatalytic flow-through H_2O_2 detector connected to an electrochemical analyzer (ALS 611B). A single-line manifold for the FIA system was made from a 0.5 mm diameter PTFE tube with a distance of 40 cm between the injection valve and the UOx-CF-reactor and

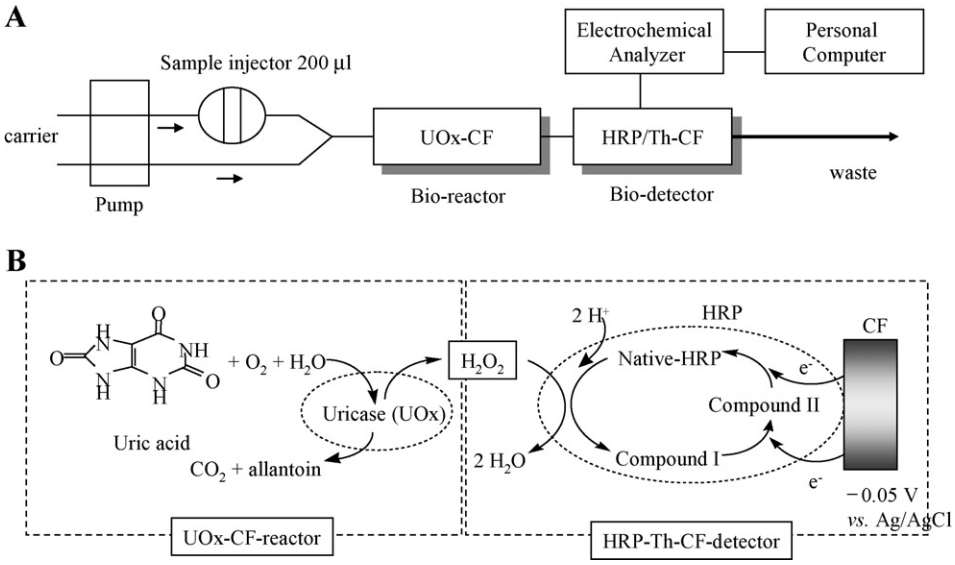

Fig. 1. (A) Schematic diagram of the UOx-CF and the HRP/Th-CF-coupled FIA biosensor for uric acid. (B) Detection scheme for uric acid by the present FIA biosensor.

5 cm between the UOx-CF reactor and the HRP/Th-CF detector. Before the measurements were taken, air-saturated 0.1 M phosphate buffer (pH 8.0) was injected at 1.9 ml/min for 1000 s to remove weakly adsorbed species. After the background current of the detector had reached steady-state values at −0.05 V vs. Ag/AgCl, uric acid standard solutions were injected and the cathodic peak current responses based on the HRP-catalyzed electro-reduction of H_2O_2 produced via UOx-catalyzed oxidation of the uric acid were recorded (Fig. 1 B). All FIA experiments were carried out at laboratory ambient temperature (22–24 °C). Throughout this experiment, the applied potential to the HRP/Th-CF-based detector was set at −0.05 V vs. Ag/AgCl because this potential is suitable for obtaining a greater current ratio of the peak current versus the background current [25] and to avoid direct electrochemical oxidation of ascorbic acid, which causes interference. As reported previously, at this detection potential, we measured the cathodic current based on the direct electron-transfer between HRP intermediates (compounds I and II) and the CF electrode surface (not the mediated current of co-adsorbed Th) [26] (see Fig. 1B).

2.5. Assay of uric acid in human serum and urine samples

Control human serum (Wako Pure Chemicals) was used as the serum sample. Human urine samples were collected without preservation and assayed within 5 h after the time of collection. Urine samples were collected from healthy male volunteers (students of our university aged 21–23 that provided informed consent). All urine samples were collected within 2 h after food intake. For determination of uric acid in these real samples using the present biosensor, serum and urine were diluted 100 times and 1000 times, respectively, using the carrier (air-saturated 0.1 M phosphate buffer, pH 8.0). Both real samples were filtered through a 0.45-μm membrane filter (Advantec, Dismic-3cp), and a 200 μL portion of the sample was injected. After a calibration curve was established, the diluted real samples were injected. A commercially available Urate-C test kit (Wako Pure chemicals) was manually used for the determination of uric acid in the same serum and urine samples (diluted 10 times). This kit contains uricase, ascorbate oxidase, peroxidase and color-producing reagent, and uric acid can be spectrophotometrically detected at 550 nm. The analytical results were compared with those obtained by the UOx-CF and HRP/Th-CF-coupled flow-biosensor.

3. Results and discussion

3.1. Optimization of UOx-adsorption conditions

Although some UOx-based biosensors have employed various immobilization matrices for UOx (e.g., polyaniline [8]; eggshell membrane [9]; a layer-by-layer polyelectrolyte film [10]; a Langmuir–Blodgett film [11]; an epoxy-resin-biocomposite membrane [12]; and a sol–gel matrix [17]), there has been little study of the direct physical adsorption of UOx on an electrode surface (especially carbon electrodes).

In general, protein adsorption onto the surface is a complex process involving various interactions, such as hydrogen bonding, electrostatic interactions, hydrophobic interactions, and van der Waals interactions. Thus, various factors such as the pH and ionic strength of the adsorption solution, surface chemistry, and surface morphology can affect protein adsorption situations.

Given these considerations, we first optimized the pH of the adsorption solution to obtain larger responses. Because phosphate buffer is the most commonly used buffer at physiological pH, the pH was controlled by using a 0.1 M phosphate buffer (KH_2PO_4/K_2HPO_4) over the pH range from pH 5.0 to 9.0. Although the buffer capacity of phosphate buffer at acidic and alkaline pH regions (i.e., pH 5 and 9, in this case) is weak, we confirmed that the pH of the UOx-dissolved solutions was not changed during the adsorption period.

The catalytic activity of the adsorbed UOx on the CF surface was evaluated by measuring the cathodic peak current to 10 μM uric acid by the UOx-CF and HRP/Th-CF-coupled flow-biosensor (see Fig. 1B). As can be seen in Fig. 2A, among examined pH levels (from pH 5.0 to 9.0), the neutral pH region (pH 6.0–8.0) seemed to be preferable for obtaining greater catalytic activity, and the largest activity was obtained at pH 7.0, although the optimum pH of the catalytic activity of free UOx (from *candida* sp.) is reported to be pH 8.5 [5]. This result implies that the pH of the adsorption solution affects not only the structure and activity of the UOx but also the interfacial properties of the adsorbed UOx-layer on the CF surface (e.g., amount, orientation and conformation of the adsorbed UOx).

Electrochemical impedance spectroscopy (EIS) is useful for studying the interfacial properties of surface-modified electrodes [27]. In the present case, the surface coverage of the adsorbed UOx on the UOx-CF surface can be evaluated by EIS, assuming that (1) the

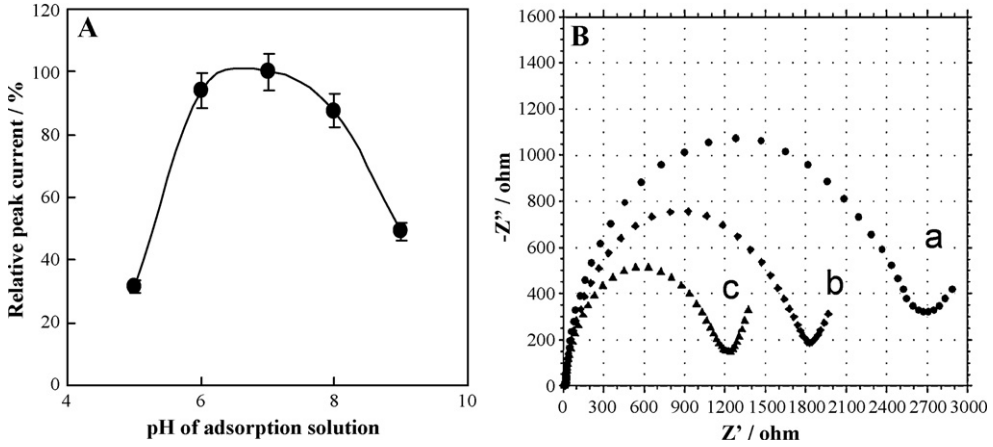

Fig. 2. (A) Effect of the pH of the UOx adsorption solution upon the relative peak current responses to 10 μM uric acid. 0.1 M phosphate buffer containing UOx (0.5 mg ml) was used as an adsorption solution. Adsorption time was 30 min. Air-saturated 0.1 M phosphate buffer (pH 8.0) was used as the carrier at a flow rate of 1.9 ml/min. The applied potential was −0.05 V vs. Ag/AgCl and (B) Nyquist plot of the EIS of UOx-adsorbed CFs. The pH values of the adsorption solutions are (a) 5, (b) 7 and (c) 9. EIS measurements were carried out after the measurements of peak currents. Deoxygenized 0.1 M phosphate buffer (pH 8.0) containing 0.25 mM hydroquinone was used as an electrolyte solution. The applied potential was set at the formal potential of the redox system (i.e., 0.05 V vs. Ag/AgCl). The frequency is from 0.01 Hz to 10 kHz.

electroactive species (in this case, hydroquinone/*p*-quinone) can directly diffuse to bare spots on the CF through pores and defects in the adsorbed UOx layer; and (2) the electroactive species can permeate through the adsorbed UOx layer and react at the CF surface. Nyquist plots of EIS for UOx-CF prepared from pH 5.0, 7.0 and 9.0 solutions are displayed in Fig. 2B. The electron transfer resistance (R_{ct}) at the electrode surface, which can be estimated by the Nyquist diameter, is a useful parameter for evaluating the interfacial properties of protein-adsorbed electrode surfaces [27]. The estimated R_{ct} value of the UOx-CF prepared at pH 5.0 (curve a, ≈2800 Ω) was larger than that for the materials prepared at pH 7.0 (curve b, ≈1900 Ω) and 9.0 (curve a, ≈1300 Ω).

It was reported that maximum adsorption occurs at the pH near the isoelectric point (p*I*) of the protein, where the net charge of the protein is zero and the protein molecule is in its most compact form [28,29]. The p*I* of UOx (from *candida* sp.) is reported to be pH 5.6 [5]. Thus, the observed EIS results for the surface coverage of the adsorbed UOx are reasonable. Although the detailed structure of the adsorbed UOx-layer (e.g., orientation, conformational relaxation and multilayer build-up formation) cannot be characterized by this EIS data, it is reasonable to say that the surface coverage of the adsorbed UOx-layer is significantly affected by the solution pH and that larger surface coverage of the adsorbed UOx is not necessarily favorable for the apparent activity of the adsorbed UOx on the CF surface. Synergistic effects of pH on the activity and structure of the UOx and on its adsorption behavior would explain this result.

It has also been reported that buffer type and buffer concentration have significant effects on protein adsorption [30]. Thus we next examined the effect of the type of buffer used for UOx adsorption. Four kinds of 0.1 M buffers (i.e., phosphate buffer, Tris–HCl buffer, Britton–Robinson buffer and borate buffer) were examined with the pH maintained at pH 7.0. As shown in Fig. 3A, the order of magnitude of the relative peak current responses to 10 μM uric acid (average of five consecutive injections) was as follows: phosphate buffer (100%, RSD = 1.35) > Britton–Robinson buffer (96%, RSD = 2.26) > Tris–HCl buffer (70%, RSD = 0.27) > borate buffer (61%, RSD = 1.01). Inorganic ions, metal ions and ionic species present in the buffer solutions might interact with not only the UOx molecule but also the CF surface, which would influence both the activity and the adsorption phenomena of the UOx. Based on this result, we selected phosphate buffer as the UOx-adsorption solvent.

Because the type of buffer affected the activity of the adsorbed UOx on the CF, we considered that buffer concentration could also affect UOx-adsorption behavior. Therefore we examined the effect of buffer concentration using three

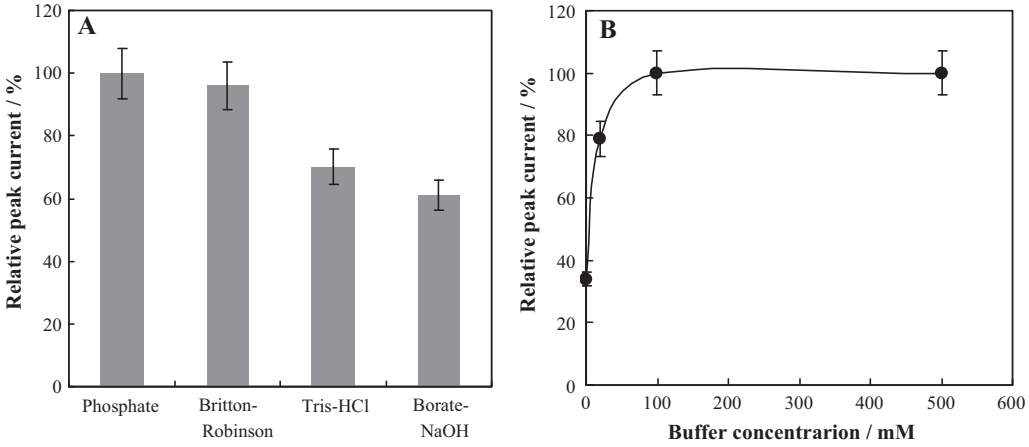

Fig. 3. (A) Effect of UOx adsorption solution buffer type on the relative peak current response to 10 μM uric acid. 0.1 M phosphate, Britton–Robinson, Tris–HCl and Borate buffers were used. The UOx concentration was fixed at 0.5 mg ml and the adsorption time was 30 min and (B) effect of the UOx adsorption solution buffer concentration on the relative peak current response to 10 μM uric acid. Phosphate buffer was used. The measurement conditions are the same as those in Fig. 2A.

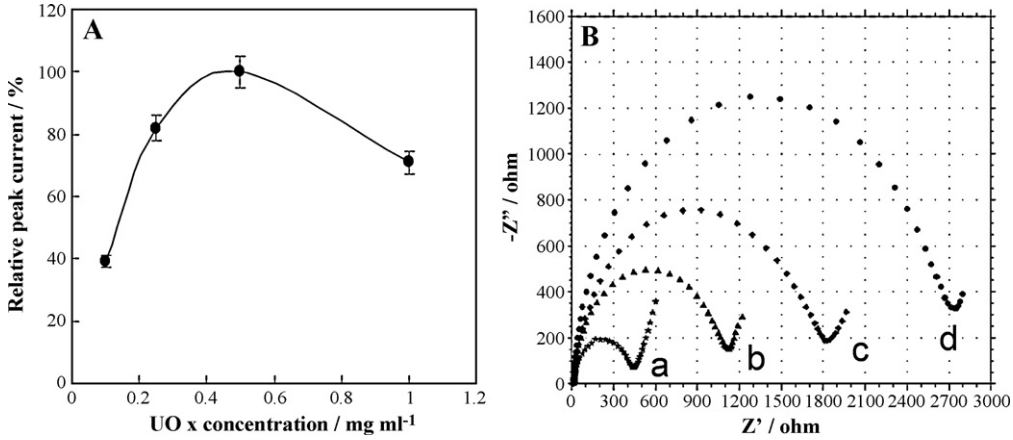

Fig. 4. (A) Effect of adsorption solution UOx concentration on the relative peak current responses to 10 μM uric acid. 0.1 M phosphate buffer (pH 7.0) was used as an adsorption solution and the adsorption time was 30 min. The measurement conditions for the peak current are the same as those in Fig. 2A and (B) Nyquist plots of the EIS of UOx-adsorbed CFs. UOx concentrations are (a) 0.1, (b) 0.25, (c) 0.5 and (d) 1 mg ml. The EIS measurement conditions are the same as those in Fig. 2B.

phosphate buffer concentrations (0, 20, 100 and 500 mM). Fig. 3B shows the comparison of the peak current responses, which were evaluated as the catalytic activities of the UOx-CF reactor. The activity of the adsorbed UOx tended to increase as the concentration of the phosphate buffer increased from 0 to 100 mM, and the activities of the UOx-CF prepared at 100 and 500 mM buffer concentrations seemed to be nearly the same.

The effect of ionic strength on protein adsorption is rather complex [28,29]. In some cases, protein adsorption is enhanced at high ionic strength due to the reduction of lateral electrostatic repulsion between the adsorbed protein molecules, which leads to increased protein density on the surface. However, inversely, the adsorption amount of lysozyme on modified agarose gels (at pH 7.4, p*I* of the lysozyme) decreased with increasing ionic strength.

The estimated R_{ct} value of the UOx-CF prepared at higher buffer concentrations was larger than that of the UOx-CF prepared at a lower concentration. These results suggest that at higher buffer concentrations, the conformational stability of the adsorbed protein may be enhanced, which would lead to an increase in the amount of active UOx molecule on the CF surface.

In our previous study, we reported that the activity of the adsorbed HRP on the CF was significantly influenced by the HRP concentration in the adsorption solution, and a higher HRP concentration (0.3–1 mg ml) was found to be unsuitable for obtaining a larger peak current response to H_2O_2 [25]. Other researchers also have reported that the structure of the protein (human serum albumin) adsorbed on a hydrophobic surface is significantly influenced by the bulk protein concentration [31]. Therefore, we next investigated the effect of the UOx concentration in the adsorption solution. The UOx was dissolved in 0.1 M phosphate buffer (pH 7.0), and the adsorption time was fixed at 30 min. Fig. 4A shows the relationship between the UOx concentration in the UOx-adsorption solution and the cathodic peak current response to 10 μM uric acid. The magnitude of the peak current to uric acid increased with increasing UOx concentration up to 0.5 mg ml and then decreased at 1 mg ml. Nyquist plots of UOx-CFs prepared from UOx solutions of various concentrations are shown in Fig. 4B. These EIS results indicate that a higher UOx bulk concentration in the UOx adsorption solution leads to larger surface coverage of the adsorbed UOx layer on the CF surface. Comparing the results at 0.5 and 1 mg ml of UOx, it is supposed that the larger amount of adsorbed UOx is not necessarily preferable for a larger response. A higher bulk protein concentration produces dense and thin layers of protein on the hydrophobic surface [31]. Other literature suggests that compact packing and/or multilayer-formation tend to cause the deactivation of adsorbed enzymes in which lateral interactions between the adjacent adsorbed enzymes likely drive a structural transition process [32]. Thus, the interfacial properties of the adsorbed UOx (i.e., surface coverage, layered structure and molecular-packing conditions) influence the catalytic activity of the adsorbed UOx on the CF. Based on these results, we selected 0.5 mg ml as the optimum UOx concentration for adsorption.

Finally, we studied the effect of adsorption time (5, 30 and 60 min) using 0.1 M phosphate buffer (pH 7.0) containing UOx (0.5 mg ml). With an increase in the adsorption time from 5 to 30 min, the catalytic activity of the UOx-CF also increased, but nearly the same activities were observed for the 30 and 60 min adsorptions (data not shown). The R_{ct} values of the UOx-CF prepared with 30 and 60 min adsorption times were also the same (ca. 1900 Ω). These results imply that the UOx adsorption kinetics are fast, and that the CF was nearly saturated within 30 min under the present adsorption conditions.

Although the detailed surface-morphology, coverage and structure of the adsorbed UOx layer on the CF surface are not clear at the present stage, overall we determined the optimized adsorption conditions as follows: 0.1 M phosphate buffer at pH 7.0, a UOx concentration of 0.5 mg ml, and an adsorption time of 30 min.

3.2. Optimization of the operational conditions

Because this uric acid biosensor is a UOx and HRP-coupled system, the activities of both enzymes should influence the response. As shown in Fig. 1B, H_2O_2 produced by the UOx-catalyzed oxidation of uric acid in the UOx-CF reactor is detected amperometrically at the HRP/Th-CF-based flow detector. Thus, in order to optimize the operational conditions, we first examined the effect of the carrier pH on the peak current response to uric acid.

Fig. 5A shows the effect of the carrier pH on the peak current responses to uric acid and H_2O_2. The pH was adjusted by using a 0.1 M phosphate buffer. Although the capacity of the phosphate buffer is weak at acidic and alkaline regions (in this case, pH 5.0 and pH 9.0), we confirmed that the pH was not changed during the experiment. As shown by the solid circles, the response to uric acid was considerably influenced by the carrier pH, and a slight alkaline condition (pH 8.0) seemed to be preferable. In the slightly acidic region (pH 5.0 and 6.0), however, the response to uric acid is less than 10% of that at pH 8.0. In contrast, in the case of the response to H_2O_2, a slightly acidic pH seemed to be preferable (pH 6.0 showed the maximum response), probably due to the broad pH dependency of HRP activity [33]. The optimum pH for the UOx (free enzyme)

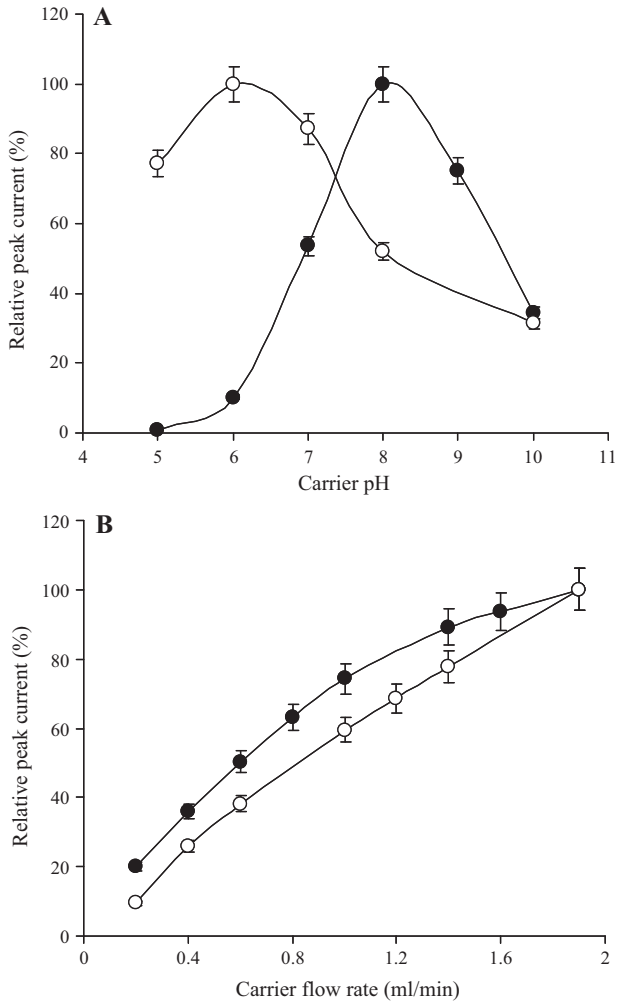

Fig. 5. (A) Effect of carrier pH on the relative peak current responses to 10 μM uric acid (●) and 10 μM H_2O_2 (○). Air-saturated 0.1 M phosphate buffer (pH 8.0) was used as the carrier at a flow rate of 1.9 ml/min. The applied potential is −0.05 V vs. Ag/AgCl and (B) effect of carrier flow rate on the relative peak current responses to 10 μM uric acid (●) and 10 μM H_2O_2 (○). Air-saturated 0.1 M phosphate buffer (pH 8.0) was used as the carrier.

used in this study is pH 8.5 [5], and since this uric acid biosensor is a UOx–HRP-coupled system, it should be safe to assume that the activity of the UOx-CF reactor primarily determines the response to uric acid. Accordingly, we selected 0.1 M phosphate buffer (pH 8.0) as the carrier solution.

Carrier flow rate is one of the important factors that influence the analytical performance of an FIA biosensor. The theory of flow electrolysis on a porous electrode has been reported [34], and the local limiting current (*iL*) of the porous electrode was given by

$$iL = RnFCV \quad (1)$$

where *n* is the number of electrons transferred per molecule, *F* is the Faraday constant, *C* is the local concentration of the electroactive species and *V* is the specific flow rate, i.e., the volume flow through a unit of cross-sectional area of the electrode. Here, *R* is the conversion efficiency, given by

$$R = 1 - \exp(-msaL/V) \quad (2)$$

where *m* is the mass transfer coefficient, *s* is the specific surface area, *a* is the cross-sectional surface area of the electrode and *L* is the length of the electrode. From these equations, it can be understood that the limiting current of the porous electrode in a flow-through

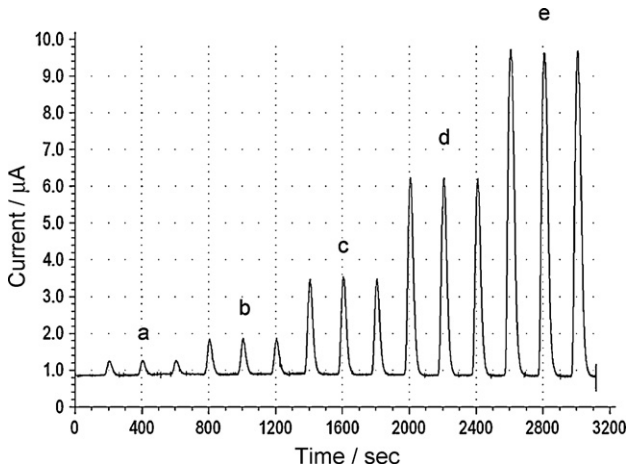

Fig. 6. Typical peak current responses to various concentrations of uric acid standard solutions. Uric acid concentrations: a, 1; b, 3; c, 10; d, 30; and e, 100 μM. Air-saturated 0.1 M phosphate buffer (pH 8.0) was used as the carrier at a flow rate of 1.9 ml/min. The applied potential is −0.05 V vs. Ag/AgCl.

detector should essentially be proportional to the carrier flow rate, which differs from disk electrodes.

Thus, we next investigated the effect of the carrier flow rate on the peak current responses to uric acid and H_2O_2. The carrier flow rate was varied in the range from 0.4 to 1.9 ml/min (1.9 ml/min is the maximum limit of the pump used in this study). As shown in Fig. 5B, the peak current responses to both uric acid and H_2O_2 increased with increasing carrier flow rate. These results imply that the rate of the enzymatic oxidation of uric acid by the UOx-CF and the rate of the bioelectrocatalytic reduction of H_2O_2 by the HRP/Th-CF are both sufficiently fast, and mass transport (*i.e.*, uric acid, oxygen and H_2O_2) limits the response of this uric acid biosensor.

3.3. Analytical performance of the uric acid biosensor

Under the optimized operational conditions (carrier flow rate of 1.9 ml/min and carrier pH of 8.0), we evaluated the analytical performance of the UOx-CF and HRP/Th-CF-coupled flow-biosensor for uric acid. Fig. 6 illustrates typical peak current responses to various concentrations of uric acid. As can be seen, the reproducibility of the response to the same concentrations of samples seems to be good. The RSDs ($n = 3$) varied from 0.16 to 2.17. The peak width was in the range of ca. 35–110 s. Thus the sample throughput was in the range of ca. 30–90 samples/h. The peak currents were found to be linear over the concentration range from 0.3 to 20 μM with a sensitivity of 0.25 μA/μM (correlation coefficient, $r^2 = 0.9968$). The lower detection limit was found to be 0.18 μM (S/N = 3, noise level 15 nA). These analytical parameters (i.e., sensitivity, detection limit and linear calibration range) of the electrochemical FIA uric acid biosensor are superior to those of other uricase/peroxidase-coupled bienzyme electrochemical uric acid biosensors (e.g., UOx/peroxidase bilayer-modified tin(IV) oxide electrode, 5 μM [13]; poly(*o*-aminophenol)-modified bienzyme carbon paste electrode, 3 μM [14]; microperoxidase modified mixed self-assembled monolayer and UOx-combined Au electrode, 2 μM [15]; and UOx/HRP-coupled fluorimetric fiber optic biosensor, 0.89 μM [18]; and chemiluminescence biosensor chip based on a microreactor, 0.6 μM [20]) and almost comparable to the UOx/peroxidase-coimmobilized Teflon membrane-based urate biosensor, 0.1 μM [16]. However, the sensitivity of the present uric acid sensor is inferior to that of a fluorescent-based UOx–peroxidase sol–gel biosensor, 0.02 μM [17] and a UOx–peroxidase coupled sepharose column based luminol chemiluminescence system, 0.08 μM [19]. In our flow biosensor system, however, a decrease in the sample

Table 1
Analytical results of uric acid in body fluids.

Sample	Sensor[a]		Spectrophotometry[b]
	[uric acid] (mM)	RSD (%) $n = 3$	[uric acid] (mM)
Serum A	0.23 ± 0.007	3.23	0.20
Serum B	0.34 ± 0.01	3.12	0.31
Urine A	3.3 ± 0.06	1.89	3.1
Urine B	2.7 ± 0.05	1.99	2.8
Urine C	3.8 ± 0.05	1.53	3.6

[a] Sample was diluted by 0.1 M phosphate buffer (pH 8.0). Dilution ratios of the serum and urine samples were 100 and 1000 times, respectively.
[b] Sample was diluted ten times by using phosphate buffer (pH 6.4) provided from the Urate-C test kit.

injection volume (e.g., 200–50 μl) may result in the expansion of its linear range.

The electrochemical Lineweaver–burk double reciprocal plot is given by

$$I = I_{\max}[\text{uric acid}]/(K_m^{app} + [\text{uric acid}]) \quad (3)$$

The apparent K_m^{app} and $I_{\max}$ were estimated to be 22.9 μM and 8.81 μA, respectively, based on the equation $Y = 2.5898X + 0.1168$ ($r^2 = 0.9989$).

3.4. Determination of uric acid in human serum and urine samples

We applied the present uric acid biosensor to real sample analysis. Human serum and urine samples were diluted 100 and 1000 times, respectively, using the carrier buffer (0.1 M phosphate buffer at pH 8.0), and injected three consecutive times.

The analytical results were compared with those obtained using a commercially available colorimetric uric acid analysis kit. Table 1 shows the comparison of the analytical results for the human serum and urine obtained by the present flow-biosensor and with conventional enzyme (uricase/peroxidase)-based spectrophotometry. As can be seen, the analytical results obtained by the present sensor seem to be in fairly good agreement with the standard spectrophotometric method. The determined uric acid concentrations in human serum were close to the average serum uric acid level (0.12–0.42 mM) [1]. Since this sensor has sufficient sensitivity for uric acid in highly diluted body fluids (100–1000 times), the electrochemical interference of ascorbic acid can be avoided, resulting in the accurate measurement of uric acid in human body samples.

3.5. Stability and reproducibility

Operational stability is an important parameter of flow biosensor systems, especially for on-line analysis applications. As reported previously, the HRP/Th-CF-based flow-detector exhibited excellent operational stability for repetitive injections of H_2O_2 (repetitive 100 sample injection of 100 μM H_2O_2 induced no serious current decrease, and the RSD was 0.41–1.21% ($n = 100$) [24]. Consecutive injections of 10 μM uric acid standard solutions (15 samples) in the new biosensor resulted in stable responses (the RSD was 0.55, $n = 10$). Therefore, it can be reasonably assumed that serious desorption and inactivation of adsorbed UOx is negligible at least during the continuous measurement period (up to 3 h).

In order to evaluate the intra-day precision (between-lot variation) of UOx-CF, three UOx-CFs were prepared in the same manner in the same day, and the peak current responses to 10 μM uric acid (five consecutive injections) were measured. In order to reduce the effect of the between-lot variation of the HRP/Th-CF detector, we used the same HRP/Th-CF detector throughout this validity-check experiment. As reported previously, the HRP/Th-CF-based flow-through detector exhibited an excellent operational stability [24]. The RSD value ($n = 3$) for the peak current response to uric acid obtained by different UOx-CF-reactors was 3.2%, indicating that the present physical adsorption protocol of the UOx-CF has acceptable reliability.

Because the activities of both the UOx-CF and HRP/Th-CF reflect the total response of the present flow-biosensor, we also evaluated the inter-day precision of the present biosensor. The RSD of the peak current responses to 10 μM uric acid was 4.84% ($n = 4$). Therefore, it can be safe to say that the enzyme-adsorbed CF-reactor and detector-coupled flow-biosensor has acceptable reproducibility even though the preparation protocol is quite easy and simple, which is one of its notable advantages.

Storage stability was also checked. When not in use, the UOx-CF was stored in 0.1 M phosphate buffer (pH 8.0) at 4 °C in the refrigerator. The HRP/Th-CF was prepared every time because the fabrication reproducibility of the HRP/Th-CF is acceptable (5.7%, $n = 3$). Unfortunately, the UOx-CF exhibited ca. 81% of its original activity after 3 days of storage. Moreover, the activity of the UOx-CF was decreased to ca. 63% after 7 days.

In order to confirm the interfacial properties of the UOx-CF (i.e., amount and structure of adsorbed UOx), we checked the change in the surface resistance evaluated by the Nyquist diameter of the EIS. Although the R_{ct} value on the initial day was ca. 1500 Ω, the R_{ct} value gradually increased during the storage period (3rd day, ca. 1800 Ω and 7th day, ca. 3000 Ω). These results suggest that the reduced storage stability of the UOx-CF may mainly be caused by unfavorable conformational changes (e.g., spreading and/or unfolding) of the adsorbed UOx on the CF surface and not desorption (leaching) from the CF surface. Thus, some appropriate additives (e.g., conformational tightening reagents) and/or entrapment of UOx in a polymer matrix and/or chemical modification of UOx on the CF surface could be useful for improving its storage stability, and such studies are currently underway in our laboratory.

4. Conclusion

In this work, we have developed a simple and relatively highly sensitive enzyme-adsorbed CF-based flow-biosensor for uric acid. The UOx-adsorbed CF (UOx-CF) was used as a column-type reactor and was combined with a highly sensitive bioelectrocatalytic flow detector for H_2O_2 using HRP/Th-coadsorbed CF (HRP/Th-CF). The adsorption conditions for UOx and the operational conditions of the UOx-CF and HRP/Th-CF-coupled uric acid flow biosensor were optimized. The resulting UOx-CF and HRP/TH-CF-coupled flow-biosensor allowed continuous, reproducible and highly sensitive determination of uric acid within the concentration range between 0.3 μM and 20 μM. The stable response (good operational stability) of this sensor may be originated from the strong affinity of both UOx and HRP on the CF surface. Furthermore, the biosensor allowed the accurate determination of uric acid in human serum and urine. Improvement of the storage stability of the UOx-CF is now underway in our laboratory.

Acknowledgement

This research was financially supported in part by the Open Research Center Project of the Ministry of Education, Science and Culture of Japan.

References

[1] W.S. Waring, D.J. Webb, S.R.J. Maxwell, Uric acid as a risk factor for cardiovascular disease, Q. J. Med. 93 (2000) 707–713.
[2] J.J. Carroll, H. Coburn, R. Douglass, A.L. Babson, A simplified alkaline phosphotungstate assay for uric acid in serum, Clin. Chem. 16 (1970) 191–194.
[3] P.A. Simkin, Isolation and quantification of serum uric acid by adsorption chromatography, Clin. Chem. 16 (1970) 191–194.

[4] M.A. Ross, Determination of ascorbic acid and uric acid in plasma by high-performance liquid chromatography, J. Chromatogr. B 657 (1994) 197–200.
[5] L. Jianguo, L. Gaoxiang, L. Hong, Z. Xiukai, Purification and properties of uricase from *Candida* sp. and its application in uric acid analysis in serum, Appl. Biochem. Biotech. 47 (1994) 57–63.
[6] P. Fossati, L. Prencipe, G. Berti, Use of 3,5-dichloro-2-hydroxybenzensulfonic acid/4-aminophenazone chromogenic system in direct enzymic assay of uric acid in serum and urine, Clin. Chem. 26 (1980) 227–231.
[7] J. Galbán, Y. Andreu, M.J. Almenara, S. de Marcos, J.R. Castillo, Direct determination of uric acid in serum by a fluorometric-enzymatic method based on uricase, Talanta 54 (2001) 847–854.
[8] J. Kan, X. Pan, C. Chen, Polyaniline-uricase biosensor prepared with template process, Biosens. Bioelectron. 18 (2004) 1635–1640.
[9] Y. Zhang, G. Wen, Y. Zhou, S. Shuang, C. Dong, M.M. Choi, Development and analytical application of an uric acid biosensor using an uricase-immobilized eggshell membrane, Biosens. Bioelectron. 22 (2007) 1791–1797.
[10] M.L. Moraes, U.P.R. Filho, O.N. Oliveira, M. Ferreira, Immobilization of uricase in layer-by-layer films in amperometric biosensors for uric acid, J. Solid state Electrochem. 11 (2007) 1489–1495.
[11] X. Wang, F. Yin, Y. Tu, A uric acid biosensor based on Langmuir–Blodgett film as an enzyme-immobilizing matrix, Anal. Lett. 43 (2010) 1507–1515.
[12] J. Arora, S. Nandwani, M. Bhambi, C.S. Pundir, Fabrication of dissolved O_2 metric uric acid biosensor using uricase epoxy resin biocomposite membrane, Anal. Chim. Acta 647 (2009) 195–201.
[13] T. Tatsuma, T. Watanabe, Oxidase/peroxidase bilayer-modified electrodes as sensors for lactate, pyruvate, cholesterol and uric acid, Anal. Chim. Acta 242 (1991) 85–89.
[14] E. Miland, A.J. Miranda Ordieres, P. Tuñón Blanco, M.R. Smyth, C.Ó. Fágáin, Poly(*o*-aminophenol)-modified bienzyme carbon paste electrode for the detection of uric acid, Talanta 43 (1996) 785–796.
[15] S. Beheraa, C. Retna Raj, Mercaptoethylpyrazine promoted electrochemistry of redox protein and amperometric biosensing of uric acid, Biosens. Bioelectron. 23 (2007) 556–561.
[16] E. Akylimaz, M.K. Segintürk, E. Dinçkaya, A biosensor based on urate oxidase-peroxidase coupled enzyme system for uric acid determination in urine, Talanta 61 (2003) 73–79.
[17] D. Martinez-Pérez, M.L. Ferrer, C.R. Mateo, A reagentless fluorescent sol–gel biosensor for uric acid detection in biological fluids, Anal. Biochem. 322 (2003) 238–242.
[18] Z. Gong, Z. Zhang, Fiber optic biosensor for uric acid based on immobilized enzymes, Anal. Lett. 29 (1996) 695–709.
[19] H.C. Hong, H.J. Huang, Flow injection anlysis of uric acid with a uricase- and horseradish peroxidase-coupled sepharose column based luminol chemiluminescence system, Anal. Chim. Acta 499 (2003) 41–46.
[20] Y. Lv, Z. Zhang, F. Chen, Chemiluminescence biosensor chip based on a microreactor using carrier air flow for determination of uric acid in human serum, Analyst 127 (2002) 1176–1179.
[21] K. Kato, K. Kano, T. Ikeda, Electrochemical characterization of carbon felt electrode for bulk electrolysis and for biocatalyst-assisted electrolysis, J. Electrochem. Soc. 147 (2000) 1449–1453.
[22] Y. Wang, Y. Hasebe, Carbon felt-based biocatalytic enzymatic flow-through detectors: Chemical modification of tyrosinase onto amino-functionalized carbon felt using various coupling reagents, Talanta 79 (2009) 1135–1141.
[23] Y. Wang, Y. Hasebe, Acridine orange-induced signal enhancement effect of tyrosinase-immobilized carbon-felt-based flow biosensor for highly sensitive detection of monophenolic compounds, Anal. Bioanal. Chem. 399 (2011) 1151–1162.
[24] Y. Hasebe, R. Imai, M. Hirono, S. Uchiyama, Carbon felt-based bioelectrocatalytic flow detectors: highly sensitive amperometric determination of hydrogen peroxide using adsorbed peroxidase and thionine, Anal. Sci. 23 (2007) 71–74.
[25] Y. Wang, Y. Hasebe, Carbon-felt-based bioelectrocatalytic flow-detectors: optimization of the adsorption conditions of horseradish peroxidase and thionine onto carbon-felt for highly sensitive amperometric determination of H_2O_2, Anal. Sci. 27 (2011) 401–407.
[26] Y. Wang, Y. Hasebe, Carbon-felt-based bioelectrocatalytic flow-detectors: role of ultrasound irradiation during the adsorption of horseradish peroxidase and thionine for highly sensitive amperometric determination of H_2O_2, Anal. Sci. 27 (2011) 605–612.
[27] Q. Chi, J. Zhang, J.U. Nielsen, E.P. Friis, I. Chorkendorff, G.W. Canters, et al., Molecular monolayer and interfacial electron transfer of Pseudomonas aeruginosa Azurin on Au(111), J. Am. Chem. Soc. 122 (2000) 4047–4055.
[28] J.K. Luey, J. Mcguire, R.D. Sproull, The effect of pH and NaCl concentration on adsorption of β-lactoglobulin at hydrophilic and hydrophobic surfaces, J. Colloid Interf. Sci. 143 (1991) 489–500.
[29] T.S. Tsapikouni, Y.F. Missirliks, pH and ionic strength effect on single fibrinogen molecule adsorption on mica studied with AFM, Colloid Surface B 57 (2008) 89–96.
[30] T. Wei, S. Kaewtathip, K. Shing, Buffer effect on protein adsorption at liquid/solid interface, J. Phys. Chem., C 113 (2009) 2053–2062.
[31] N.B. Sheller, S. Petrash, M.D. Foster, Atomic force microscopy and X-ray reflectivity studies of albumin adsorbed onto self-assembled monolayers of hexadecyltrichlorosilane, Langmuir 14 (1998) 4535–4544.
[32] A. Sethuraman, G. Vedantham, T. Imoto, T. Przybycien, G. Belfort, Protein unfolding at interfaces: slow dynamics of α-helix to β-sheet transition, Proteins: Struct. Funct. Bioinf. 56 (2004) 669–678.
[33] K.G. Paul, Peroxidases. in: P.B. Boyer (Ed.), The Enzymes, vol. 8, Academic Press, New York, 1963, pp. 227–237.
[34] R.E. Shioda, K.B. Keating, in: A.J. Bard (Ed.), Electroanalytical Chemistry, vol. 12, Dekker, New York, 1982, pp. 19–27.